Effect of Internal Energy on the Repulsive Coulomb Barrier of Polyanions

Daniel A. Horke, Adam S. Chatterley, and Jan R. R. Verlet*

Department of Chemistry, University of Durham, DH1 3LE Durham, United Kingdom

(Received 14 October 2011; published 24 February 2012)

The nature of the repulsive Coulomb barrier in isolated molecular polyanions is studied by means of the photodetachment dynamics of the S_1 excited state of the fluorescein dianion which is bound solely by the repulsive Coulomb barrier. Photoelectron spectra reveal a feature at a constant electron kinetic energy, regardless of the excitation energy. This is explained by using an adiabatic tunneling picture for electron loss through successive repulsive Coulomb barriers correlating to vibrationally excited states. This physical picture is supported by time-resolved photoelectron spectra, showing that the tunneling lifetime is also invariant with excitation energy.

DOI: 10.1103/PhysRevLett.108.083003 PACS numbers: 33.80.Eh, 33.60.+q

Isolated molecular polyanions have attracted significant interest because of their electronic structure [1–5]. An inherent degree of instability arises from the repulsion between the negatively charged sites on the molecular skeleton. As a result, many polyanions common in the condensed phase, such as SO_4^{2-}, have not been observed in the gas phase [6]. Yet, the same interactions can also lead to a dramatic increase in electronic stability. A potential barrier is present due to the balance between the short-range attraction and long-range electron-anion repulsion, which can prevent an excess electron from escaping [7–10]. This repulsive Coulomb barrier (RCB) can lead to exotic observations such as polyanions with negative electron binding energies [11,12]. The RCB height can be related to the distance between localized charge sites, effectively providing an intramolecular ruler [8]. Photoelectron (PE) spectroscopy coupled with electrospray ionization provides a route to understanding molecular polyanions, as the PE emission is sensitive to the RCB [3]. At low electron kinetic energy (eKE), there is an energetic cutoff below which the PE can be emitted only by tunneling through the RCB [5,7,10,13]. Above the RCB, the PE trajectory is guided by the anisotropic RCB [14,15]. Despite the many important consequences of the RCB, there have been no detailed studies on the dependence of the RCB on internal energy of the polyanion and its effect on the tunneling process.

For a given electronic state, there is not simply a single RCB. Instead, every rovibrational level will, in principle, have an RCB associated with it. An important question is how the RCBs vary with internal energy and how the electron emission is affected by this high density of RCBs. In this Letter, we report on the adiabatic tunneling of an electronically excited state of a molecular polyanion that is bound solely by an RCB. Using a combination of PE spectroscopy and time-resolved PE spectroscopy [16,17], we show that there exists an RCB for every vibrational state and that electron loss via tunneling through the RCB conserves the vibrational energy. Our results provide detailed insight into the nature of the RCB and the dynamics of electron loss from polyanions.

Experiments are performed on the doubly deprotonated fluorescein dianion $[\mathrm{fl}-2\mathrm{H}]^{2-}$, the structure of which is shown Fig. 1(a). In solution, $[\mathrm{fl}-2\mathrm{H}]^{2-}$ has a bright $S_1 \leftarrow S_0$ transition around 2.5 eV that decays predominantly by fluorescence, with a quantum yield of 0.92 [18]. Recently, McQueen *et al.* showed that isolated $[\mathrm{fl}-2\mathrm{H}]^{2-}$ does not fluoresce [19]. Instead, excitation of the S_1 state leads to loss of an electron. This was used to determine the intrinsic absorption spectrum by monitoring the yield of $[\mathrm{fl}-2\mathrm{H}]^{-}$. Although it is not surprising that an electron is lost following $S_1 \leftarrow S_0$ excitation in $[\mathrm{fl}-2\mathrm{H}]^{2-}$, it is unclear if the S_1 state is completely

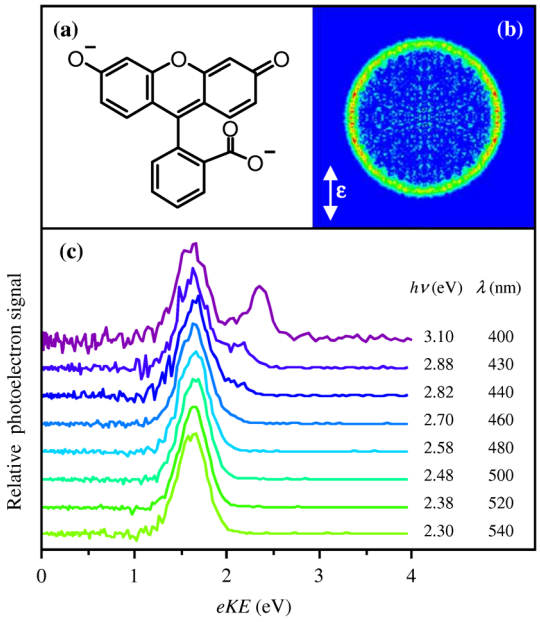

FIG. 1 (color online). PE spectra of the doubly deprotonated fluorescein dianion, with its chemical structure shown in (a). (b) Deconvoluted PE image taken at 2.48 eV (500 nm) and (c) resultant PE spectra taken over a 0.8 eV energy range.

unbound with respect to electron loss or if it is bound by a RCB. Here, we show that the S_1 state is bound by the RCB and utilize it as a probe to explore the dependence of the RCB on internal energy.

The experiments were performed by using our recently developed femtosecond PE imaging spectrometer [20,21]. Mass-selected $[\mathrm{fl}-2\mathrm{H}]^{2-}$ is generated from a 1 mM solution of fluorescein in methanol ($p\mathrm{H}\sim 11$ through the addition of NaOH) in an electrospray ionization source that is coupled to a time-of-flight mass spectrometer. Following mass selection, the $[\mathrm{fl}-2\mathrm{H}]^{2-}$ ion packet is perpendicularly intersected with radiation from a tunable nanosecond (ns) laser or by pump and probe pulses from a femtosecond (fs) laser system. The nanosecond pulses are generated by a Nd:YAG pumped optical parametric oscillator producing $\sim$5 mJ pulse^{-1} across the visible. Femtosecond pulses are generated from a commercial Ti:sapphire amplified laser system. Pump pulses around 500 nm are generated by using an optical parametric amplifier and by mixing the signal output with residual 800 nm in a beta-barium borate crystal. A portion of the fundamental 800 nm is used as probe pulses, and the two are delayed relative to each other by using a motorized delay stage. The temporal resolution is $\sim$140 fs based on a cross correlation in a thin beta-barium borate crystal. The interaction point between ions and laser is at the center of a PE spectrometer. For ns and fs single color experiments, the intensities in the interaction region are $I_{\mathrm{ns}}\sim 7\times 10^{6}$ and $I_{\mathrm{fs}}\sim 1\times 10^{10}$ W cm^{-2}, respectively. For pump-probe experiments, fs beams were loosely focused to an intensity of $I_{\mathrm{pu}}\sim 8\times 10^{11}$ and $I_{\mathrm{pr}}\sim 5\times 10^{12}$ W cm^{-2}. The emitted PE cloud is guided in the direction mutually perpendicular to the laser and ion beam onto a position sensitive detector, by using a velocity-map imaging arrangement [22]. The point at which a PE strikes the detector is monitored by using a CCD, and the resultant PE images are analyzed by using the polar onion peeling method [23]. This provides PE spectra and PE angular distributions. Spectra have been calibrated to the known spectrum of I^-, and the spectrometer has a spectral resolution of $\frac{\Delta E}{E}=5\%$.

Figure 1(b) shows a deconvoluted PE image taken at 2.48 eV (500 nm) with a ns laser. It reveals a single, slightly anisotropic feature ($\beta_2=-0.2\pm 0.1$). The PE spectra of $[\mathrm{fl}-2\mathrm{H}]^{2-}$ taken with a ns laser at various excitation wavelengths between 2.30 (540 nm) and 2.88 eV (430 nm) are shown in Fig. 1(c). Also shown is a PE spectrum taken at 3.10 eV (400 nm) with the fs laser. There is no apparent difference between PE spectra at a given excitation energy taken with the fs or ns laser, confirming that the observed PEs arise from the absorption of a single photon [24].

The most striking aspect of the data in Fig. 1(c) is that a feature with $e\mathrm{KE}=1.64$ eV is seen in all the PE spectra. Ordinarily in PE spectroscopy, the electron binding energy (eBE) is defined as $e\mathrm{BE}=h\nu-e\mathrm{KE}$. Despite increasing the photon energy by $\sim$0.8 eV from 540 to 400 nm, there is no concomitant increase in eKE. This suggests that the eBE is increasing with increasing photon energy, which is unphysical. At photon energies above 2.60 eV (480 nm), an additional feature can be identified in the PE spectrum. At 2.70 eV (460 nm), this appears as a small shoulder to the main feature and extends to higher eKE as the photon energy is increased. It also gains intensity relative to the PE feature at 1.64 eV. Fitting the PE spectra with a Gaussian for each feature reveals that the higher eKE feature shifts by an amount equal to the increase in photon energy. Hence, this feature behaves as expected in PE spectroscopy, and its eBE is constant.

To gain further insight, we have also performed femtosecond time-resolved experiments in which the $S_1\leftarrow S_0$ transition is excited and the ensuing S_1 dynamics probed by using 1.55 eV (800 nm) light at variable delays. In Fig. 2(a), representative PE spectra are shown when the probe arrives before the pump ($t<t_0$) and when they are temporally overlapped ($t\sim t_0$). The $t<t_0$ PE spectrum is identical to a pump-only spectrum. The additional PE features at high eKE arise from multiphoton processes, as the laser pulses used in the time-resolved studies are focused into the interaction region [25]. In the PE spectrum at $t\sim t_0$, a new PE feature can be identified around 2.9 eV.

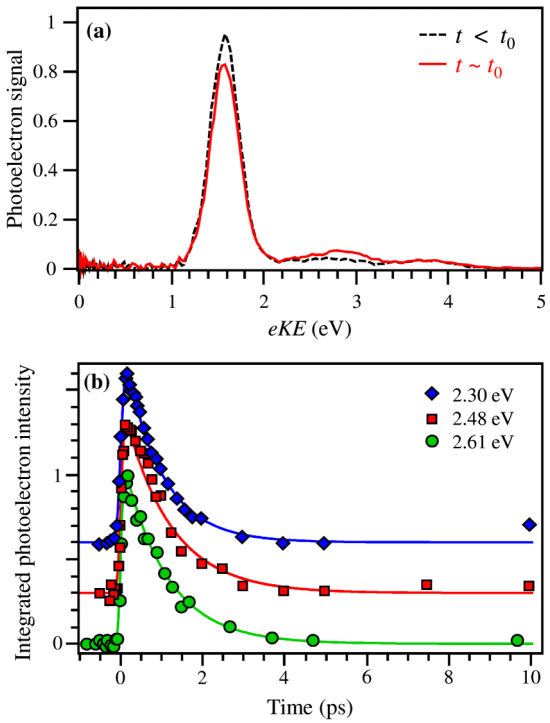

FIG. 2 (color online). Time-resolved PE spectra following excitation to S_1. (a) Representative PE spectra when pump and probe pulses are temporally overlapped and when the pump arrives after the probe. (b) Integrated PE signal of the S_1 feature at three different excitation energies, indicating an invariance of the lifetime with respect to excitation energy.

This corresponds to the removal of an electron from the S_1 state by the probe photon. With increasing delay, the pump-probe feature decays in intensity. In Fig. 2(b), the integrated PE counts are plotted as a function of time for three different excitation energies: 2.30 (538 nm), 2.48 (500 nm), and 2.61 eV (475 nm). Each data set is well reproduced by using a single exponential decay with time constants of $\tau = 0.9$, 1.1, and 1.1 ± 0.2 ps, respectively. These experiments have been repeated at lower light intensities, yielding similar results.

The time-resolved PE spectra clearly show that the PE feature at $e\mathrm{KE} = 1.64$ eV is not due to direct photodetachment, because, on the time scale of our experiment, this would be instantaneous. Instead, the S_1 state is bound by an RCB, and the lifetime observed for the S_1 state corresponds to the tunneling lifetime of the electron through the RCB [26]. The short lifetime indicates that the S_1 state is likely to be close to the top of the RCB. In order to explain the fact that the PE feature arising from tunneling does not shift in eKE, we consider that the total energy must be conserved. The eKE of the PE can be expressed as $e\mathrm{KE} = h\nu - \mathrm{ABE} - E_{\mathrm{int}}$, where ABE is the adiabatic binding energy (difference in energy between the dianion and anion in their ground state geometries) and E_{int} is the internal energy of the anion. Accordingly, the observed invariance of eKE in Fig. 1(c) must be accompanied by a change in E_{int} as the photon energy is changed. In normal PE spectroscopy, photodetachment is a vertical transition, and the E_{int} is determined by the Franck-Condon factors in going from the dianion to anion [3]. For $[\mathrm{fl} - 2\mathrm{H}]^{2-}$ excited to the S_1 state, electron loss is not a vertical transition.

For a dianion A^{2-}, each vibrational level of product A^- will have an associated RCB leading to the formation of A^{2-}. The RCB can be viewed either from the perspective of the dianion (inner RCB) or from the perspective of an electron approaching the anion (outer RCB) [27]. In Fig. 3(a), two scenarios are depicted for the overall shape of the RCB: (i) The height of the outer RCB is constant while the inner RCB increases with E_{int}, or (ii) the inner RCB is constant while the height of the outer RCB decreases with E_{int}. Wang, Ding, and Wang have presented arguments favoring the latter [7], but if this is the case, then, for photon energies that exceed the inner RCB height, direct detachment is the only open channel for electron loss. This is not observed, because at *all* photon energies in Fig. 1(c), a PE feature due to tunneling appears at $e\mathrm{KE} = 1.64$ eV. Invoking a constant outer RCB height for every vibrational level allows the observed PE spectra to be fully understood.

With reference to Fig. 3(b), vertical excitation to the lowest part of the S_1 band at 2.30 eV leads to tunneling through an RCB that correlates adiabatically to a low vibrational level of $[\mathrm{fl} - 2\mathrm{H}]^-$. Note that, in principle, the RCB leading to the S_1 state is not the same as that leading to the S_0, as shown in Fig. 3(b) [28]. They are

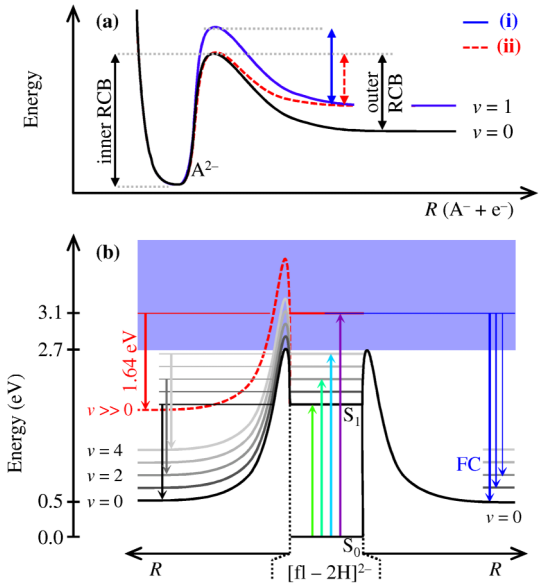

FIG. 3 (color online). Effect of internal energy on RCB. (a) shows two scenarios in which the height of the outer RCB is (i) constant or (ii) changes with internal energy. The case for the fluorescein dianion is shown in (b), where R is the $[\mathrm{fl} - 2\mathrm{H}]^-$ to $e-$ distance. The RCBs correlating to the S_0 state (right) and to the S_1 state (left) are shown. With increasing excitation energy, and hence internal energy in S_1, there is a progression of RCBs correlating to $[\mathrm{fl} - 2\mathrm{H}]^-$ with higher internal energy. Tunneling through these RCBs leads to PEs with constant kinetic energy (downward arrows), as shown on the left-hand side. Once above the RCB for S_0, a direct detachment channel opens up leading to a PE spectrum determined by the Franck-Condon factors between the dianion in its S_0 state and the monoanion in its D_0 state. This is shown on the right-hand side for excitation at 3.10 eV.

identical at long range, as both RCBs share the same final product state $[\mathrm{fl} - 2\mathrm{H}]^-$. Differences are only expected to arise at very short range, and, hence, we anticipate that the height of the S_1 outer RCB is similar to that of the S_0 outer RCB.

Increasing the photon energy beyond 2.30 eV accesses higher vibrational levels in the S_1 state. If E_{int} is conserved during tunneling, then $[\mathrm{fl} - 2\mathrm{H}]^-$ will be formed vibrationally excited, resulting in a constant eKE. When the excitation energy is sufficient to overcome the inner RCB between the S_0 state and the final product state $[\mathrm{fl} - 2\mathrm{H}]^-$, a new electron loss channel opens up, as direct photodetachment into the continuum becomes possible. This is indicated on the right side of Fig. 3(b) and occurs between $2.58\ \mathrm{eV} < h\nu < 2.70$ eV. For photon energies above 2.70 eV, direct detachment is a vertical transition, and the E_{int} of the product $[\mathrm{fl} - 2\mathrm{H}]^-$ is determined by the Franck-Condon factors between the dianion and anion, which are independent of excitation energy. Concomitant to direct detachment, $h\nu > 2.70$ eV is still resonant with the $S_1 \leftarrow S_0$ transition, exciting high vibrational levels of the S_1 state. Even at a photon energy of 3.10 eV, more than

0.4 eV in the continuum above the RCB for direct detachment from the $S_0(v = 0)$ state, the S_1 state preferentially tunnels adiabatically through the RCB corresponding to its internal energy. As this state is above a continuum, nonadiabatic autodetachment may be expected to compete, but this would appear as a broadening of the PE feature towards higher eKE. The PE spectrum at 3.10 eV shows no evidence for this. Hence, the emerging physical picture is one in which there is a dense progression of potential energy surfaces, each corresponding to a vibrational (and rotational) level of the anion. The effective height of the outer RCB is approximately constant.

Further evidence for the validity of this conceptual picture can be gained from time-resolved PE spectroscopy. If the outer RCB has the same height regardless of E_{int}, then the RCB experienced by the electron at a given excitation energy may be expected to have a similar shape. This is consistent with the observation that the lifetime for tunneling does not vary significantly over a 0.3 eV window. The tunneling lifetime should be very sensitive to changes in barrier height and width, as the tunneling probability scales exponentially with these variables.

The direct detachment feature provides a measure of the adiabatic binding energy, which we estimate to be ABE = 0.5 ± 0.1 eV. Based on the onset of this feature and the ABE, the outer RCB height of the S_0 state can be estimated to be approximately 2.1–2.2 eV.

This physical picture of a series of vibrational potential energy surfaces also explains tandem mass spectra of $[\text{fl} - 2\text{H}]^{2-}$ [19]. Following $S_1 \leftarrow S_0$ photoexcitation, an electron is lost leading to $[\text{fl} - 2\text{H}]^{-}$. For thermal activation methods, such as off-resonance irradiation collisionally activated dissociation or infrared multiphoton dissociation, electron loss may be expected to be a facile mechanism as ABE = 0.5 eV. This is, however, not observed, and instead dissociation with loss of the CO_2^- group is favored [19]. As vibrational energy is imparted to $[\text{fl} - 2\text{H}]^{2-}$, the electron is prevented from escaping because the inner RCB is increasing with increasing E_{int}. Dissociation in favor of electron loss is a common feature of tandem mass spectrometry using activation methods through collisions or photons [29,30].

In conclusion, we have presented the first detailed study of the dependence of an RCB on internal energy. This is done by using an excited state bound solely by the RCB which is probed by PE spectroscopy in the frequency and time domain. A PE feature that arises from tunneling of the excited state through the RCB is observed at eKE = 1.64 eV, regardless of the excitation energy used. This can be accounted for by invoking a physical picture in which every vibrational level has an RCB associated with it and the height of the outer RCB is approximately constant for all vibrational levels. This is supported by time-resolved PE spectroscopy experiments, which reveal that the tunneling lifetime is insensitive to excitation energy, suggesting that the barrier width and height are similar at all energies. This picture remains valid also above the lowest RCB, and tunneling can be seen in parallel to direct detachment into the continuum. Electron loss by tunneling through the RCB is strongly adiabatic and can be viewed as a diagonal transition, exhibiting dramatically different behavior to direct detachment. Our results highlight the complexity of the RCB in molecular polyanions and its consequences for interpreting PE spectra. Moreover, it provides a framework in which to understand tandem mass spectrometry of polyanions.

This work has been supported by the EPSRC (EP/D073472/1) and Durham University. A. S. C. is funded by the Leverhulme Trust. We thank the EPSRC laser loan pool for loan of the ns laser system.

*j.r.r.verlet@durham.ac.uk

[1] M. K. Scheller, R. N. Compton, and L. S. Cederbaum, Science **270**, 1160 (1995).
[2] A. I. Boldyrev, M. Gutowski, and J. Simons, Acc. Chem. Res. **29**, 497 (1996).
[3] L. S. Wang and X. B. Wang, J. Phys. Chem. A **104**, 1978 (2000).
[4] A. Dreuw and L. S. Cederbaum, Chem. Rev. **102**, 181 (2002).
[5] X. B. Wang and L. S. Wang, Annu. Rev. Phys. Chem. **60**, 105 (2009).
[6] X. B. Wang, J. B. Nicholas, and L. S. Wang, J. Chem. Phys. **113**, 10 837 (2000).
[7] X. B. Wang, C. F. Ding, and L. S. Wang, Phys. Rev. Lett. **81**, 3351 (1998).
[8] L. S. Wang, C. F. Ding, X. B. Wang, and J. B. Nicholas, Phys. Rev. Lett. **81**, 2667 (1998).
[9] O. T. Ehrler, J. M. Weber, F. Furche, and M. M. Kappes, Phys. Rev. Lett. **91**, 113006 (2003).
[10] K. Matheis, L. Joly, R. Antoine, F. Lepine, C. Bordas, O. T. Ehrler, A. R. Allouche, M. M. Kappes, and P. Dugourd, J. Am. Chem. Soc. **130**, 15 903 (2008).
[11] X. B. Wang and L. S. Wang, Nature (London) **400**, 245 (1999).
[12] J. M. Weber, I. N. Ioffe, K. M. Berndt, D. Loffler, J. Friedrich, O. T. Ehrler, A. S. Danell, J. H. Parks, and M. M. Kappes, J. Am. Chem. Soc. **126**, 8585 (2004).
[13] X. B. Wang, C. F. Ding, and L. S. Wang, Chem. Phys. Lett. **307**, 391 (1999).
[14] X.-P. Xing, X.-B. Wang, and L.-S. Wang, Phys. Rev. Lett. **101**, 083003 (2008).
[15] C. G. Ning, P. D. Dau, and L. S. Wang, Phys. Rev. Lett. **105**, 263001 (2010).
[16] A. Stolow, A. E. Bragg, and D. M. Neumark, Chem. Rev. **104**, 1719 (2004).
[17] J. R. R. Verlet, Chem. Soc. Rev. **37**, 505 (2008).
[18] D. Magde, R. Wong, and P. G. Seybold, Photochem. Photobiol. **75**, 327 (2002).
[19] P. D. McQueen, S. Sagoo, H. Yao, and R. A. Jockusch, Angew. Chem., Int. Ed. **49**, 9193 (2010).

[20] J. Lecointre, G. M. Roberts, D. A. Horke, and J. R. R. Verlet, J. Phys. Chem. A **114**, 11 216 (2010).
[21] D. A. Horke and J. R. R. Verlet, Phys. Chem. Chem. Phys. **13**, 19 546 (2011).
[22] A. Eppink and D. H. Parker, Rev. Sci. Instrum. **68**, 3477 (1997).
[23] G. M. Roberts, J. L. Nixon, J. Lecointre, E. Wrede, and J. R. R. Verlet, Rev. Sci. Instrum. **80**, 053104 (2009).
[24] See Supplemental Material at http://link.aps.org/supplemental/10.1103/PhysRevLett.108.083003 for a comparison of fs and ns experiments and details of spectra fitting.
[25] The feature at 3.8 eV corresponds to two-photon resonance-enhanced photodetachment leaving $[\mathrm{fl} - 2\mathrm{H}]^-$ in its D_0 ground state, while the feature at 2.7 eV corresponds to a similar process but leading to an electronically excited state of $[\mathrm{fl} - 2\mathrm{H}]^-$.
[26] O. T. Ehrler, J. P. Yang, A. B. Sugiharto, A. N. Unterreiner, and M. M. Kappes, J. Chem. Phys. **127**, 184301 (2007).
[27] J. C. Marcum and J. M. Weber, J. Chem. Phys. **131**, 194309 (2009).
[28] A. Dreuw and L. S. Cederbaum, Phys. Rev. A **63**, 049904 (E) (2001).
[29] H. J. Cooper, K. Hkansson, and A. G. Marshall, Mass Spectrom. Rev. **24**, 201 (2005).
[30] S. Ard, N. Mirsaleh-Kohan, J. D. Steill, J. Oomens, S. B. Nielsen, and R. N. Compton, J. Chem. Phys. **132**, 094301 (2010).